Springer

KSME

Thermodynamic assessment of integrated heat recovery system combining exhaust-gas heat and cold energy for LNG regasification process in FSRU vessel[†]

Sangick Lee[1] and Byung Chul Choi[1,2,*]

[1]R&D Center, Korean Register of Shipping, Busan 618-814, Korea
[2]Department of Mechanical Engineering, Massachusetts Institute of Technology, MA 02139, USA

Abstract

A thermodynamic assessment of an integrated heat recovery system, which simultaneously recovers both the cold energy of LNG released into seawater and the exhaust gas heat of diesel generator released into ambient air during the regasification process in a LNG-FSRU vessel, has been carried out. For the LNG regasification unit consisting of two-stage heat exchangers, a primary Rankine cycle was applied as a typical power cycle of the type A for recovering cold energy to the first-stage heat exchanger. A secondary Rankine cycle of the type B was serially inserted between the first-stage and the second-stage heat exchangers for recovery of the remaining cold energy of preheated LNG. Then, in the type C, the exhaust gas, which had a relatively high temperature, was applied as the heat source of the secondary Rankine cycle, instead of seawater. In such a sequential procedure, the type C was finally suggested as an integrated heat recovery system, in which the seawater and exhaust gas were combined as the heat sources. When the net outputs produced from each heat recovery system were maximized by changing the pressure and mass flow rate of working fluid, the thermal efficiency of the integrated heat recovery system of the type C was $\eta_{I,EG} = 0.0741$. The results showed an improvement of approximately 13.3% (25.6%) in the thermal efficiency compared to the value of $\eta_{I,SW} = 0.0654$ ($\eta_I = 0.0590$) for the conventional cold energy recovery system of the type B (the type A), which only used seawater as the heat source. Based on this finding, a possibility of utilizing the integrated heat recovery system with the combined cycle within the LNG-FSRU was confirmed.

Keywords: LNG-FSRU; Heat recovery; LNG; Seawater; Exhaust gas; Rankine cycle

---

1. Introduction

The Liquefied natural gas (LNG) supply chain consists of natural gas exploration and production, liquefaction, shipping, regasification and distribution. LNG is generally produced through a liquefaction process of Natural gas (NG), which has a boiling point of approximately -162°C at atmospheric pressure. The electrical energy consumed during production processes such as chilling and pressurizing is stored as the cold energy of LNG. Many studies have been conducted to recover and reuse the available energy during the regasification processes.

Rocca [1] suggested an LNG regasification system based on a power generation cycle working with ethane to be applied in food freezing industry and in air conditioning of commercial sector far from the regasification facility. Szargut and Szczygiel analyzed a cascade system with ethane as working fluid for the production of electricity [2]. They performed an optimization with a pinch analysis of heat exchangers. An eco-nomic evaluation was conducted with the value of generated electricity and the reduction of CO_2 emission. Choi et al. [3] proposed and optimized a cascade Rankine cycle consisting of multiple stages of the organic Rankine cycle in a layered structure. It was found that the thermodynamic efficiency generally increased as the number of stages increased. Combinations of cascade stages with various working fluids were investigated for the thermal efficiency. Shi et al. [4] proposed a hybrid thermal power system integrated with the inlet air cooling, compressor inter-cooling and LNG cold energy utilization. The system consisted of a gas turbine cycle, a heat recovery steam generator, a steam turbine cycle and LNG regasification. The LNG was used both to cool the steam and to be directly expanded.

On the other hand, for the reuse of the cold energy of LNG, Kim and Ro [5] analyzed the feasibility of a combined cycle power plant with a gas turbine, a heat recovery steam generator and a steam turbine. The power augmentation was demonstrated using LNG as source of cold energy for the inlet air cooling process of gas turbine to increase the performance of plant. A heat exchanger between air and LNG was applied in the inlet chilling process instead of a refrigeration system. The
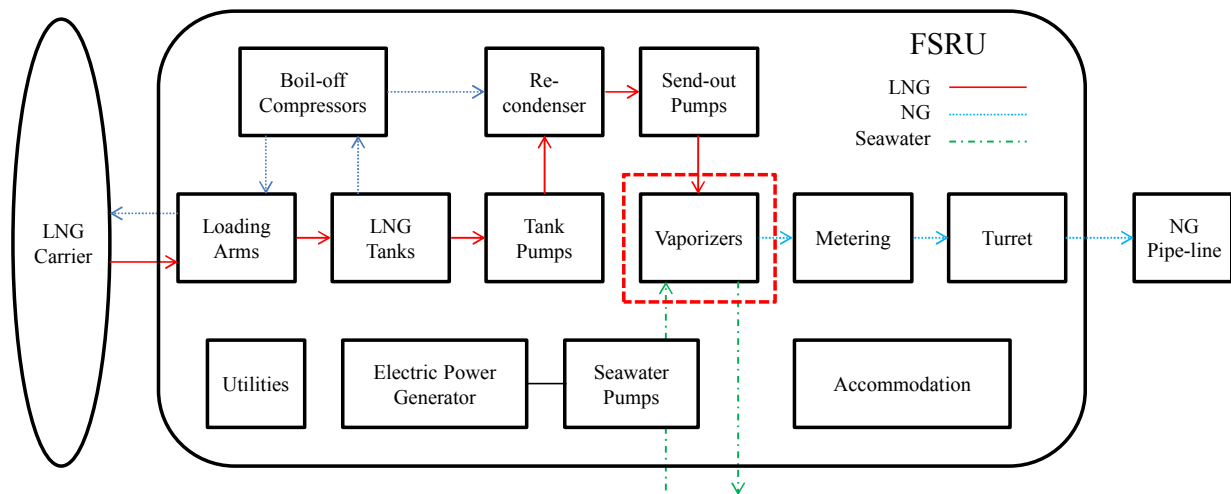
Fig. 1. Schematic of an LNG-FSRU between an LNG carrier and NG pipe-line.

concept of mirror gas turbine was proposed by Kaneko et al. [6] as a combined cycle of a conventional gas turbine and an inverted Brayton cycle. LNG was used in cooling the exhaust gas from a turbine of the inverted cycle to generate electricity with the removal of an evaporation system using seawater.

Studies that comprehensively consider low grade waste heat and renewable energy are also being conducted. Miyazaki et al. [7] developed a power generation cycle using LNG cold energy recovery cycle combined with refuse incineration. The combined cycle is based on Rankine cycle with an ammonia-water mixture as working fluid. They did parametric analysis to increase the thermal and exergy efficiencies compared to the conventional cycle. A power system was proposed to utilize the low grade waste heat with LNG as its heat sink by Wang et al. [8]. They conducted a multi-objective optimization using a genetic algorithm to maximize the thermodynamic efficiency, and minimize the economic cost of Rankine cycle power generator. Oliveti et al. [9] proposed three sequential cycles of a water-steam-closed Rankine cycle in the waste incinerator plant, an intermediate ammonia-closed Rankine cycle, and a methane-open Rankine cycle to capture the thermal energy released from an LNG regasification terminal. Dispenza et al. [10, 11] conducted a feasibility study of a combined heat and power cycle using the cryogenic stream of LNG during the regasification as a cold source in a gas turbine with helium as working fluid. Wang et al. [12] investigated the use of LNG cold energy as a heat sink to a Rankine cycle with transcritical CO_2 as working fluid employing the heat of geothermal water. Franco and Casarosa [13] modeled the direct expanding power generation of LNG. They analyzed a multistage direct expansion cycle with three pressure level configuration.

Generally, in cases of the regasification terminals on land, when LNG is unloaded from the carrier and its cold heat energy is recycled, approximately 240 kWh of electricity can be generated from the stored cold energy in 1 ton of LNG [14]. However, not enough studies have been done on the recovery

of cold energy of LNG in LNG-FSRU (Floating storage & regasification unit), a floating LNG processing facility utilizing seawater for its regasification process. When compared to LNG-FPSO's (Floating production storage & offloading), LNG-FSRU has simple topside and hull constructions for severe offshore conditions. Besides, the core processes and components for the regasification have relatively low complexity. Thus, it may be comparatively easier to explore various technical attempts with the LNG-FSRU's. Also, because the LNG-FSRU needs to produce electricity on its own, the economic values of technology to enhance the thermal efficiency of the system by recovering cold energy in the LNG-FSRU may be higher than those of on-land facilities, considering fuel transportation and power generation efficiencies. With this motivation, the cold energy of LNG regasification and the low grade heat of exhaust gas wasted from its electric power generators were defined as limited quantities in an LNG-FSRU with practically feasible design specification. We also investigated the availability of an integrated heat recovery system with a combined cycle of the exhaust gas and LNG through a thermodynamic approach.

2. FSRU vessel

2.1 LNG regasification process

As shown in the schematic in Fig. 1, LNG is unloaded from LNG carriers to storage tanks through loading arms. The stored LNG is regasified using the heat of seawater to be transported to onshore through metering, turrets, and pipelines. The pressurizing and condensation of boil-off gas is also included in the LNG-FSRU. A large capacity generator is necessary for providing electricity not only for the LNG regasification process but also for the on-board utilities and the accommodations for crews of the vessel.

The basic capacity of processing LNG of the FSRU used in the present study is consistently set at 198.26 kg/s (approximately 800 mmSCFD) [15]. Table 1 shows the chemical

Table 1. Chemical composition of the LNG.

LNG composition	Mole fraction
Methane (CH_4)	0.9133
Ethane (C_2H_6)	0.0536
Propane (C_3H_8)	0.0214
i-Butane (i-C_4H_{10})	0.0047
n-Butane (n-C_4H_{10})	0.0046
i-Pentane (i-C_5H_{12})	0.0001
n-Pentane (n-C_5H_{12})	0.0001
Nitrogen (N_2)	0.0022

composition of LNG [3]. The initial and final temperatures of LNG are defined as -165°C and 0°C, respectively. The inlet and outlet temperatures of seawater for the heat of regasification are fixed at 15°C and 5°C, respectively [3]. In addition, two diesel generators, with a maximum output of 8.55 MW each, are installed to provide electricity required for the LNG regasification and the ship operation. They generate 12.825 MW of electricity together at all times by concurrently operating at 75% load in normal operation mode [15]. From the generators, a total of 26.8 kg/s of exhaust gases with a temperature of 351°C is released into ambient air [16].

2.2 Thermodynamic cycles for the energy recovery

Fig. 2 shows process diagrams of three types (A, B and C) of thermodynamic cycles for recovering waste heats released from the FSRU vessel. First, P-100 pump shown in Fig. 2(a) (Type A) increases the pressure of LNG_1 in 0.50 MPa to the pressure of LNG_2 in 5.00 MPa. Then, LNG_2 is preheated to LNG_3 through the first-stage heat exchanger within a primary Rankine cycle. The primary Rankine cycle consists of a

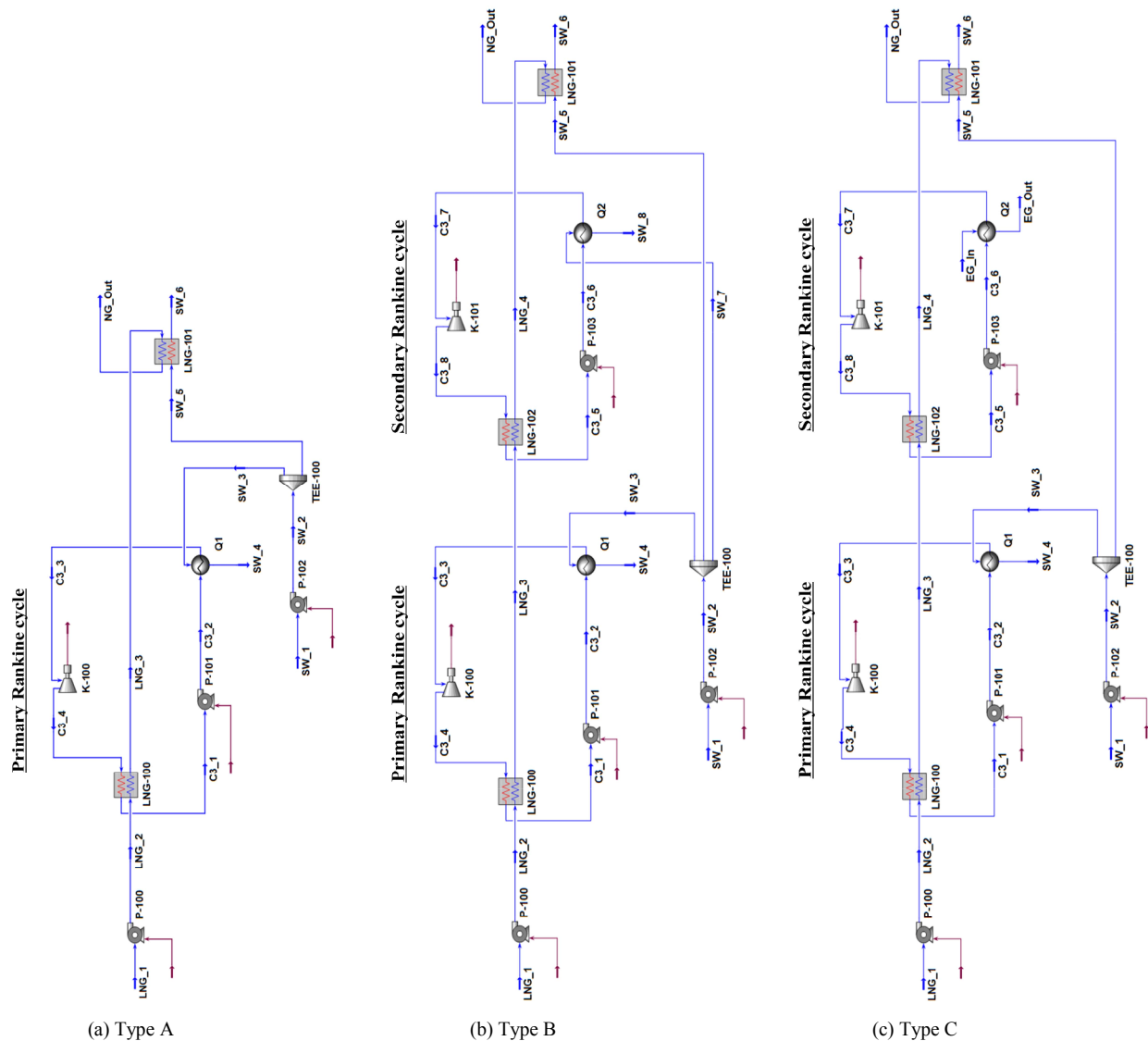(a) Type A   (b) Type B   (c) Type C

Fig. 2. Process diagram for the heat recovery systems consisted of (a) type A: The primary Rankine cycle and the secondary Rankine cycle with; (b) type B: Seawater or; (c) type C: Exhaust gas in the LNG regasification.

typical Rankine cycle which uses propane as its working fluid. So, P-101 pump increases pressure, and vaporization is carried out by Q1 vaporizer using seawater as its heat source. The pressurized and vaporized working fluid produces electricity with expansion work in K-100 turbine and is resupplied to the pump after being reliquefied at low temperature and low pressure through heat exchanges with LNG at the first-stage heat exchanger. In the next stage, the preheated LNG of LNG_3 is produced as natural gas of predetermined specification through reheating by seawater at the second-stage heat exchanger of LNG-101.

To enhance the electricity production rate from the waste heat, a secondary Rankine cycle in serial type has been employed. In Fig. 2(b) (Type B), the secondary Rankine cycle consists of P-103 pump, Q2 vaporizer, K-101 turbine, and LNG-102 condenser. It uses the temperature difference between the preheated LNG after the primary Rankine cycle and seawater to produce additional electricity with the same working fluid of propane. On the other hand, Fig. 2(c) (Type C) considers an increase of temperature difference within the cycle by replacing SW_7 and SW_8, which is the inlet and outlet of seawater as a heat reservoir, with the exhaust gas of the generator EG_In and EG_Out, which has a heat source of limited capacity with higher temperatures, in the secondary Rankine cycle. To produce natural gas with a certain specification, the output of the secondary Rankine cycle, the heating of LNG_4 is commonly controlled by the second-stage heat exchanger.

2.3 Calculation condition

For the modelling and thermodynamic analysis of LNG regasification processes, a commercial simulation tool of Aspen HYSYS (ver. 7.3) was used with the Peng-Robinson Equation of State, which is known to provide a prediction with relatively high accuracy for thermodynamic properties of hydrocarbons, including LNG [17-19]. The thermodynamic properties were calculated on a basis of the energy balance of the each mechanical component under the steady-flow condition with the mass balance, as given in Eq. (1).

$$\dot{Q} - \dot{W} = H_{out} - H_{in} = \dot{m}(h_{out} - h_{in}), \tag{1}$$

where the changes in the kinetic and potential energies were negligible.

In investigating the thermodynamic performance of waste heat recovery systems applied to the regasification process of the constant capacity, the restraints shown in Table 2 were applied. In this estimation, the qualities of working fluids at inlets of pumps C3_1 and C3_5, and the outlets C3_2 and C3_6 were restricted to $x = 0$ (no vapor). The inlets of turbines C3_3 and C3_7 were also restricted to $x = 1$ (no liquid). On the other hand, the efficiencies of turbines and pumps were fixed at 0.75 each, and it was assumed that the power generated at the turbine would be directly converted into electricity

Table 2. Constraint conditions on maximum outputs of the power cycles.

Condition	Constraint
Quality of C3_1, C3_2, C3_5, C3_6	$x = 0$
Quality of C3_3, C3_7	$x = 1$
Efficiencies of pumps and turbines	0.75
Seawater	Pure H_2O
Exhaust gas	Heated air (79% N_2 and 21% O_2)
Temperature of C3_1	-150.00°C
Temperature of C3_3	10.00°C
Temperature of C3_7 in case of the seawater	10.00°C
Temperature of C3_7 in case of the exhaust gas	346.00°C

without any loss.

As heat sources, seawater was treated as a pure H_2O and exhaust gas was treated as heated air. Plate-fin type heat exchangers were used for counterflow LNG, and shell-tube type heat exchangers were used for seawater and exhaust gas in evaporators of Rankine cycles. Heat losses from the heat exchangers were neglected. In addition, for the inlets and outlets of the heat exchangers, temperatures were fixed at the following values: C3_1 = −150°C, C3_3 = 10.00°C, seawater case: C3_7 = 10.00°C, and exhaust gas case: C3_7 = 346.00°C. Overall, all pressure and heat losses within pipes of the processes were neglected.

3. Results and discussion

3.1 Primary Rankine cycle

When the primary Rankine cycle is in operation alone, the output of K-100 turbine $\dot{W}_{K-100}$, the power of P-101 pump $\dot{W}_{P-101}$, and the power of P-102 pump $\dot{W}_{P-102}$ for supplying seawater to the first and second stage heat exchangers are given as the following Eqs. (2)-(4).

$$\dot{W}_{K-100} = \dot{m}_{C3\_3}\left(h_{C3\_3} - h_{C3\_4}\right), \tag{2}$$

$$\dot{W}_{P-100} = \dot{m}_{C3\_1}\left(h_{C3\_2} - h_{C3\_1}\right), \tag{3}$$

$$\dot{W}_{P-102} = \dot{m}_{SW\_1}\left(h_{SW\_2} - h_{SW\_1}\right). \tag{4}$$

Therefore, the net output $\dot{W}_{net1}$ produced from the primary Rankine cycle while the LNG with a constant mass flow rate is gasified into NG can be defined as Eq. (5) given below.

$$\dot{W}_{net1} = \dot{W}_{K-100} - \dot{W}_{P-101} - \dot{W}_{P-102}. \tag{5}$$

In this regard, when the mass flow rate of working fluids at C3_3, the inlet of K-100, was fixed at 197.22 kg/s as the maximum value satisfying the conditions of Table 2, the power characteristics of Eqs. (2)-(5) with the change of C3_3 pressure are shown in Fig. 3. As the P-101 pump increased the pressure at the inlet of K-100 turbine from 0.15 to 0.60 MPa,
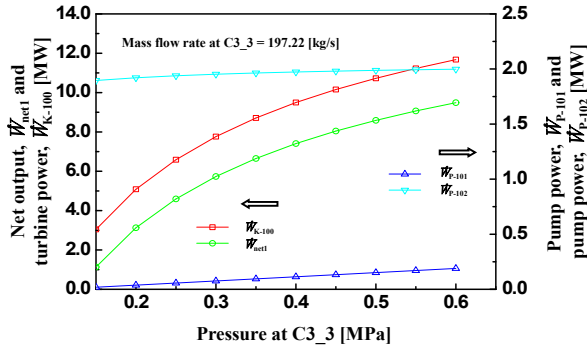
Fig. 3. Turbine power of K-100 ($\dot{W}_{K-100}$), pump power of P-101 ($\dot{W}_{P-101}$), pump power of P-102 ($\dot{W}_{P-102}$), and net output ($\dot{W}_{net1}$) for the primary Rankine cycle when pressure at C3_3 is varied for a fixed mass flow rate at C3_3 = 197.22 [kg/s].

the output of turbine $\dot{W}_{K-100}$ noticeably increased from 3.045 to 11.677 MW. Here, the power consumed by the pump increased almost linearly from 0.019 to 0.190 MW, but it was lower than approximately 1.6% compared to the turbine output $\dot{W}_{K-100}$. However, the net output $\dot{W}_{net1}$ produced by the primary Rankine cycle not only increased from 1.131 to 9.489 MW as the pressure of the turbine inlet increased, but also showed a big difference in the magnitude depending on the changes in pressure of the turbine inlet. Therefore, controlling the pressure of the turbine inlet can also be an important parameter in the stability of the electric power generated by the power cycle.

On the other hand, the power of P-102 seawater pump $\dot{W}_{P-102}$ showed a slight increase of 1.896-1.998 MW with a steady trend. This indicated that it did not respond sensitively to the changes of pressure in propane, as a heat transfer medium of the intermediate loop in supplying the thermal capacity required for preheating the LNG in the first-stage heat exchanger. This also reveals that the power produced by the primary Rankine cycle, in which propane with a constant mass flow rate is vaporized by seawater and condensed by LNG, might be small in transferring the heat of seawater to the LNG. This implies that the thermodynamic efficiency of the primary Rankine cycle, applied to utilize the temperature difference of seawater and LNG, can be relatively low. This issue will be further discussed in Sec. 3.4.

To find the maximum net output of the primary Rankine cycle, a mapping was performed by changing the mass flow rate and pressure of working fluid at the turbine inlet. As results, the primary Rankine cycle showed the maximum net output when the pressure was 0.63 MPa and the mass flow rate was 196.94 kg/s at the turbine inlet C3_3. Table 3 shows the thermodynamic properties for each state in the condition. The maximum output was $max(\dot{W}_{net1})$ = 9.728 MW, which suggests that more than 75% of electricity can be replaced by the operation of the primary Rankine cycle alone, when compared to the 12.825 MW of electricity generated by the 2 diesel generators of this study.

In the following, the characteristics of the additional output

Table 3. Thermodynamic properties at each state for the maximum net power of the primary Rankine cycle applied to the LNG regasification unit.

State	Temperature [°C]	Pressure [MPa]	Mass flow rate [kg/s]	Specific enthalpy [kJ/kg]
LNG_1	-165.50	0.50	198.26	-5184.54
LNG_2	-163.23	5.00	198.26	-5171.59
LNG_3	-45.13	4.50	198.26	-4545.04
NG_Out	0	4.00	198.26	-4398.62
C3_1	-150.00	0.10	196.94	-3091.14
C3_2	-149.77	0.63	196.94	-3090.12
C3_3	10.00	0.63	196.94	-2399.94
C3_4	-39.78	0.10	196.94	-2460.39
SW_1	15.00	0.10	3807.47	-15930.96
SW_2	15.03	0.50	3807.47	-15930.44
SW_3	15.03	0.50	3137.45	-15930.44
SW_4	5.00	0.50	3137.45	-15973.76
SW_5	15.03	0.50	670.02	-15930.44
SW_6	5.00	0.50	670.02	-15973.76

produced by serially inserting a secondary Rankine cycle in front of the second-stage heat exchanger of LNG_101, were examined with all the thermodynamic states fixed at the certain condition that the primary Rankine cycle produces maximum output.

3.2 Secondary Rankine cycle with seawater

For the type B of Fig. 2(b), for the secondary Rankine cycle using seawater as its heat source, the output of K-101 turbine $\dot{W}_{K-101}$, the power of P-103 pump $\dot{W}_{P-103}$, and the power change of P-102 seawater pump $\Delta\dot{W}_{P-102}$ by the secondary Rankine cycle are given as the following Eqs. (6)-(8).

$$\dot{W}_{K-101} = \dot{m}_{C3\_7}\left(h_{C3\_7} - h_{C3\_8}\right), \tag{6}$$

$$\dot{W}_{P-103} = \dot{m}_{C3\_5}\left(h_{C3\_6} - h_{C3\_5}\right), \tag{7}$$

$$\Delta\dot{W}_{P-102} = \Delta\dot{m}_{SW\_1}\Delta\left(h_{SW\_2} - h_{SW\_1}\right). \tag{8}$$

Therefore, while the LNG is regasified into NG with the uniform specification, the net output produced by the secondary Rankine cycle with seawater as a heat source $\dot{W}_{net2,SW}$ can be defined as Eq. (9).

$$\dot{W}_{net2,SW} = \dot{W}_{K-101} - \dot{W}_{P-103} - \Delta\dot{W}_{P-102}. \tag{9}$$

Fig. 4 shows the power characteristics in accordance with Eqs. (6)-(9) when the pressure of the working fluid at the K-101 turbine inlet C3_7 is changed with its mass flow rate fixed at 33.06 kg/s. As the P-103 pump increased the pressure of K-101 turbine inlet from 0.21 to 0.57 MPa, the turbine output sharply increased in $\dot{W}_{K-101}$ = 0.062-1.185 MW, and the net
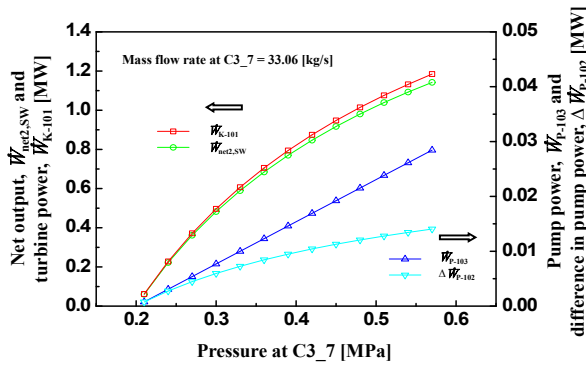
Fig. 4. Turbine power of K-101 ($\dot{W}_{K-101}$), pump power of P-103 ($\dot{W}_{P-103}$), difference in pump power of P-102 ($\Delta \dot{W}_{P-102}$), and net output of $\dot{W}_{net2,SW}$ for the secondary Rankine cycle with seawater when pressure at C3_7 is varied for a fixed mass flow rate at C3_7 = 33.06 [kg/s].

output of the secondary Rankine cycle with seawater improved in $\dot{W}_{net2,SW} = 0.060\text{-}1.142$ MW. At this time, the changes in the power of P-103 pump and the P-102 seawater pump caused by the secondary Rankine cycle were, respectively, $\dot{W}_{P-103} = 0.001\text{-}0.028$ MW and $\Delta \dot{W}_{P-102} = 0.001\text{-}0.014$ MW. The ratio of the net output of the secondary Rankine cycle to the turbine output was maintained to be almost close to unity at $\dot{W}_{net2,SW} / \dot{W}_{K-101} = 0.968\text{-}0.964$. Therefore, any additional power consumed by pumps of the secondary Rankine cycle can be ignored in comparing to the ratio of $\dot{W}_{net1} / \dot{W}_{K-100} = 0.371\text{-}0.813$ for the primary Rankine cycle.

In methods similar to the primary Rankine cycle, a mapping was performed for the secondary Rankine cycle with seawater as a heat source by changing the mass flow rate and the pressure of working fluid at the turbine inlet. The secondary Rankine cycle showed the maximum net output $max(\dot{W}_{net2,SW}) = 1.142$ MW when the pressure was 0.60 MPa and the mass flow rate was 33.06 kg/s at the turbine inlet C3_7. Table 4 shows the thermodynamic properties for each state in the condition. Therefore, for the heat recovery system applied in LNG regasification, using the double operation with a secondary Rankine cycle implies 11.74 % improvement of the maximum net output as compared to the single operation of primary Rankine cycle, of which the maximum net output $max(\dot{W}_{net1}) = 9.728$ MW.

3.3 Secondary Rankine cycle with exhaust gas

For type C of Fig. 2(c), the net output $\dot{W}_{net2,EG}$ produced by the secondary Rankine cycle, in which the exhaust gas was applied as the heat source in replacement of seawater, can be defined as Eq. (10).

$$\dot{W}_{net2,EG} = \dot{W}_{K-101} - \dot{W}_{P-103} - \Delta \dot{W}_{P-102}. \tag{10}$$

Fig. 5 shows the power characteristics of Eqs. (6)-(8) and (10) when the mass flow rate of the working fluid was changed with the inlet pressure of K-101 turbine C3_7 fixed at 19.00 MPa. As the mass flow rate of the turbine inlet increased from 5.83 to 8.61 kg/s, the turbine power output

Table 4. Thermodynamic properties at each state for the maximum net power of the secondary Rankine cycle with seawater.

| State	Temperature [°C]	Pressure [MPa]	Mass flow rate [kg/s]	Specific enthalpy [kJ/kg]
LNG_1	-165.50	0.50	198.26	-5184.54
LNG_2	-163.23	5.00	198.26	-5171.59
LNG_3	-45.13	4.50	198.26	-4545.04
LNG_4	-26.26	4.30	198.26	-4472.30
NG_Out	0	4.00	198.26	-4398.62
C3_1	-150.00	0.10	196.94	-3091.14
C3_2	-149.77	0.63	196.94	-3090.12
C3_3	10.00	0.63	196.94	-2399.94
C3_4	-39.78	0.10	196.94	-2460.39
C3_5	-35.13	0.20	33.06	-2872.46
C3_6	-34.85	0.60	33.06	-2871.53
C3_7	10.00	0.60	33.06	-2398.91
C3_8	-21.12	0.20	33.06	-2436.23
SW_1	15.00	0.10	3835.23	-15930.96
SW_2	15.03	0.50	3835.23	-15930.44
SW_3	15.03	0.50	3137.45	-15930.44
SW_4	5.00	0.50	3137.45	-15973.76
SW_5	15.03	0.50	337.18	-15930.44
SW_6	5.00	0.50	337.18	-15973.76
SW_7	15.03	0.50	360.60	-15930.44
SW_8	5.00	0.50	360.60	-15973.76
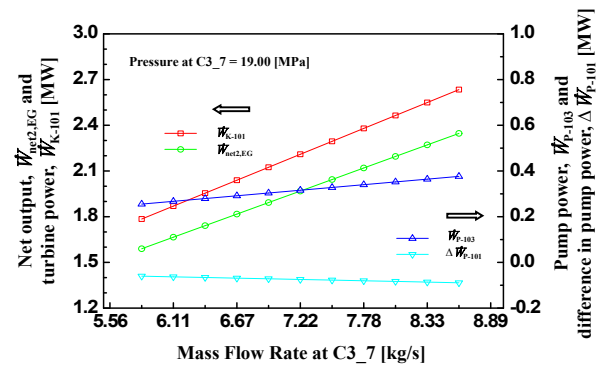
Fig. 5. Turbine power of K-101 ($\dot{W}_{K-101}$), pump power of P-103 ($\dot{W}_{P-103}$), difference in pump power of P-102 ($\Delta \dot{W}_{P-102}$), and net output of $\dot{W}_{net2,EG}$ for the secondary Rankine cycle with exhaust gas when mass flow rate at C3_7 is varied for a fixed pressure at C3_7 = 19.00 [MPa].

showed significant increase in $\dot{W}_{K-101} = 1.785\text{-}2.634$ MW. In addition, the power consumed by the P-103 pump within the secondary Rankine cycle was $\dot{W}_{P-103} = 0.255\text{-}0.376$ MW, and the change in the power of P-102 seawater pump $\Delta \dot{W}_{P-102}$ decreased from -0.060 to -0.089 MW at the same time. Thus, since the powers of pumps offset each other, the final net output of the secondary Rankine cycle with the exhaust gas increased in $\dot{W}_{net2,EG} = 1.590\text{-}2.347$ MW.

Table 5. Thermodynamic properties at each state for the maximum net power of the secondary Rankine cycle with exhaust gas.

State	Temperature [°C]	Pressure [MPa]	Mass flow rate [kg/s]	Specific enthalpy [kJ/kg]
LNG_1	-165.50	0.50	198.26	-5184.54
LNG_2	-163.23	5.00	198.26	-5171.59
LNG_3	-45.13	4.50	198.26	-4545.04
LNG_4	-37.25	4.30	198.26	-4508.02
NG_Out	0	4.00	198.26	-4398.62
C3_1	-150.00	0.10	196.94	-3091.14
C3_2	-149.77	0.63	196.94	-3090.12
C3_3	10.00	0.63	196.94	-2399.94
C3_4	-39.78	0.10	196.94	-2460.39
C3_5	-35.13	0.20	8.61	-2872.46
C3_6	-22.70	19.00	8.61	-2828.74
C3_7	346.00	19.00	8.61	-1714.36
C3_8	190.36	0.20	8.61	-2020.29
SW_1	15.00	0.10	3638.09	-15930.96
SW_2	15.03	0.50	3638.09	-15930.44
SW_3	15.03	0.50	3137.45	-15930.44
SW_4	5.00	0.50	3137.45	-15973.76
SW_5	15.03	0.50	500.64	-15930.44
SW_6	5.00	0.50	500.64	-15973.76
EG_In	351.00	0.11	26.80	333.49
EG_Out	0.48	0.10	26.80	-24.56

Mapping was performed in the same methods by changing the mass flow rate and pressure of the working fluid at the turbine inlet. Table 5 shows the thermodynamic properties for each state in the condition when the maximum net output is reached in the secondary Rankine cycle with exhaust gas as its heat source.

The maximum output of $max(\dot{W}_{net2,EG}) = 2.347$ MW was reached when the pressure was 19.00 MPa and the mass flow rate was 8.61 kg/s at the turbine inlet C3_7. Therefore, for the waste heat recovery system used in LNG regasification, application of exhaust gas as a heat source yielded an improved performance of approximately two times compared to the secondary Rankine cycle with seawater as a heat source, of which the maximum net output was $max(\dot{W}_{net2,SW}) = 1.142$ MW.

For a purpose of reference, the heat losses within the heat exchangers were neglected in these calculations. However, from a practical point of view, the changes in the heat losses, in the occurrence of the phase transition of propane, can be larger especially during the vaporization process of propane in the Q2 evaporator of the secondary Rankine cycle, since the change in temperature of the exhaust gas from the inlet to the outlet is approximately 351-0°C, and it is rather large compared to the change in the temperature of seawater, which is 15-5°C [20]. In addition, the physical characteristics of the

exhaust gas having vapor phase of relatively high temperature also involve a relatively low specific heat and density at constant pressure, as compared to those of water. This indicates the necessity for more systematic studies on the optimization of the second Rankine cycle, which simultaneously utilizes both exhaust gas and the cold energy of the preheated LNG. For more details, the next section will discuss the comparative analysis of thermodynamic efficiencies of each waste heat recovery system.

3.4 Comparison of thermodynamic efficiencies

As discussed before about the waste heat recovery systems in the LNG regasification process, the net outputs produced by the heat recovery systems of Fig. 2 showed improvements in the order of type A, B and C. This section compares the thermodynamic efficiencies of each heat recovery system with the maximum outputs by considering the 1st and 2nd laws of thermodynamics. First, the heat $\dot{Q}_{Q1}$ supplied from the seawater through the Q1 evaporator of the primary Rankine cycle, the heat of seawater $\dot{Q}_{Q2,SW}$ supplied through the Q2 evaporator of the secondary Rankine cycle, the exhaust gas heat $\dot{Q}_{Q2,EG}$, and the heat of seawater $\dot{Q}_{LNG-101}$ transferred to the LNG-101 heat exchanger to produce NG of the target specification are defined as the following Eqs. (11)-(14).

$$\dot{Q}_{Q1} = \dot{m}_{SW\_3}(h_{SW\_3} - h_{SW\_4}), \tag{11}$$

$$\dot{Q}_{Q2,SW} = \dot{m}_{SW\_7}(h_{SW\_7} - h_{SW\_8}), \tag{12}$$

$$\dot{Q}_{Q2,EG} = \dot{m}_{EG\_In}(h_{EG\_In} - h_{EG\_Out}), \tag{13}$$

$$\dot{Q}_{LNG-101} = \dot{m}_{SW\_5}(h_{SW\_5} - h_{SW\_6}). \tag{14}$$

For the three types of waste heat recovery systems, the efficiency of the 1st law of thermodynamics η_I, the efficiency of the 2nd law of thermodynamics η_{II}, and the Carnot efficiency η_C are defined as the following.

For type A:

$$\eta_I = \dot{W}_{net1} / (\dot{Q}_{Q1} + \dot{Q}_{LNG-101}) \tag{15a}$$

$$\eta_{II} = \eta_I / \eta_C = \eta_I / (1 - T_{LNG\_2} / T_{SW\_2}). \tag{15b}$$

For type B:

$$\eta_{I,SW} = (\dot{W}_{net1} + \dot{W}_{net2,SW}) / (\dot{Q}_{Q1} + \dot{Q}_{Q2,SW} + \dot{Q}_{LNG-101,SW}) \tag{16a}$$

$$\eta_{II,SW} = \eta_{I,SW} / \eta_{C,SW} = \eta_{I,SW} / (1 - T_{LNG\_2} / T_{SW\_2}). \tag{16b}$$

For type C:

$$\eta_{I,EG} = (\dot{W}_{net1} + \dot{W}_{net2,EG}) / (\dot{Q}_{Q1} + \dot{Q}_{Q2,EG} + \dot{Q}_{LNG-101,EG}) \tag{17a}$$

$$\eta_{II,EG} = \eta_{I,EG} / \eta_{C,EG} = \eta_{I,EG} / (1 - T_{LNG\_2} / T_{EG\_In}). \tag{17b}$$

The defined thermodynamic efficiencies are shown in Fig. 6 for each of the type A, B and C systems. The thermal efficiencies of the waste heat recovery systems showed increasing
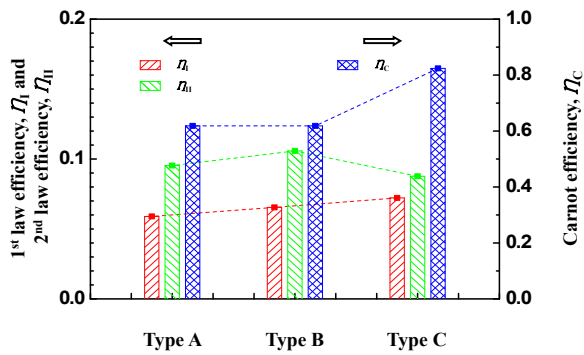
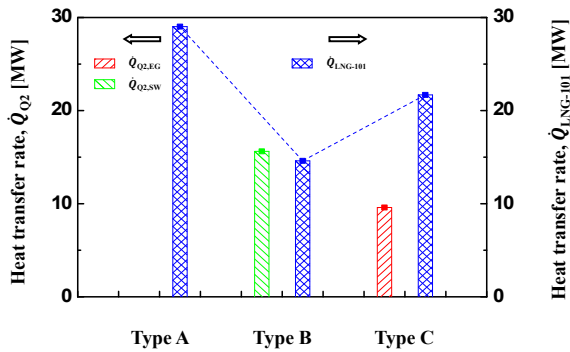Fig. 6. Comparison of thermal efficiencies among the type A, B and C.

Fig. 7. Comparison of heat transfer rate for the major heat exchangers.

trends with values of $\eta_I = 0.0590$, $\eta_{I,SW} = 0.0654$, and $\eta_{I,EG} = 0.0741$, depending on the systematic configurations of the seawater and the exhaust gas. The $\eta_{I,EG}$ for an integrated heat recovery system combining seawater and exhaust gas, showed an improvement of thermal efficiency by 13.3% in comparison with the $\eta_{I,SW}$ for the system with only seawater as its heat source. This shows that both the net output and the thermal efficiency improve when the heat of exhaust gas wasted from the FSRU vessel, which has a relatively higher temperature than that of seawater, is recovered with the cold energy of LNG.

In cases of the 2nd law of thermodynamics, the type B showed an improvement of about 11%, from $\eta_{II} = 0.0953$ to $\eta_{II,SW} = 0.1058$, as compared to the type A, however, the type C showed a decrease with a value of $\eta_{II,EG} = 0.0877$. Note that it is difficult to assign any significance on this comparison since the value of Carnot efficiency, which is defined as a function of the maximum and minimum temperatures, rises only numerically by applying the exhaust gas instead of seawater. That is, there can be differences in exergy rate fed in from the heat sources since the exhaust gas has a limited heat capacity compared to the seawater, a naturally unlimited heat reservoir [20]. Therefore, it is necessary to further study the exergy analysis.

Additionally, as shown in Fig. 7, when the $\dot{Q}_{Q1}$ has a constant value of 135.914 MW at the vaporizer of the primary Rankine cycle, the heat transfer rate of LNG-101 in the second-stage heat exchanger of the type A is $\dot{Q}_{LNG-101} = 29.025$

Table 6. Thermodynamic properties at each state for the maximum net power of the secondary Rankine cycle with exhaust gas when the working fluid of propane in the secondary Rankine cycle was replaced with R134a.

State	Temperature [°C]	Pressure [MPa]	Mass flow rate [kg/s]	Specific enthalpy [kJ/kg]
LNG_1	-165.50	0.50	198.26	-5184.54
LNG_2	-163.23	5.00	198.26	-5171.59
LNG_3	-45.13	4.50	198.26	-4545.04
LNG_4	-37.00	4.30	198.26	-4507.05
NG_Out	0.00	4.00	198.26	-4398.62
C3_1	-150.00	0.10	196.94	-3091.14
C3_2	-149.77	0.63	196.94	-3090.12
C3_3	10.00	0.63	196.94	-2399.94
C3_4	-39.78	0.10	196.94	-2460.39
C3_5	-35.13	0.20	17.22	-9051.24
C3_6	-26.77	19.00	17.22	-9033.39
C3_7	346.00	19.00	17.22	-8479.31
C3_8	193.54	0.20	17.22	-8613.95
SW_1	15.00	0.10	3633.64	-15930.96
SW_2	15.03	0.50	3633.64	-15930.44
SW_3	15.03	0.50	3137.45	-15930.44
SW_4	5.00	0.50	3137.45	-15973.76
SW_5	15.03	0.50	496.19	-15930.44
SW_6	5.00	0.50	496.19	-15973.76
EG_In	351.00	0.11	26.80	333.49
EG_Out	2.50	0.10	26.80	-22.57

MW. For type B, in which seawater is applied as an additional heat source for the secondary Rankine cycle, a heat of $\dot{Q}_{Q2,SW} = 15.621$ MW is transferred from the seawater and the value of $\dot{Q}_{LNG-101,SW}$ decreases to 14.607 MW. On the other hand, for type C supplied with the heat of $\dot{Q}_{Q2,EG} = 9.596$ MW from the exhaust heat, the heat of seawater required for the second-stage heat exchanger shows relatively less decrease as $\dot{Q}_{LNG-101,EG} = 21.688$ MW. This suggests that solutions not only to minimize the heat loss which occurs in the secondary Rankine cycle mentioned in the Sec. 3.3 but also to concurrently recover the cold energy of preheated LNG in the LNG_4 heated by the seawater of SW_5 in the second-stage heat exchanger of LNG-101 must be explored to optimize the efficiency of the waste heat recovery system combining LNG and exhaust gas.

3.5 Considerations for the working fluids

For type C, the net power $\dot{W}_{net2,EG}$ for the secondary Rankine cycle was examined by the replacement with R134a and R245fa, respectively, as the representative organic working fluids. Tables 6 and 7 show the thermodynamic properties for each state in the maximum condition.

Table 7. Thermodynamic properties at each state for the maximum net power of the secondary Rankine cycle with exhaust gas when the working fluid of propane in the secondary Rankine cycle was replaced with R245fa.

State	Temperature [°C]	Pressure [MPa]	Mass flow rate [kg/s]	Specific enthalpy [kJ/kg]
LNG_1	-165.50	0.50	198.26	-5184.54
LNG_2	-163.23	5.00	198.26	-5171.59
LNG_3	-45.13	4.50	198.26	-4545.04
LNG_4	-36.42	4.30	198.26	-4504.84
NG_Out	0.00	4.00	198.26	-4398.62
C3_1	-150.00	0.10	196.94	-3091.14
C3_2	-149.77	0.63	196.94	-3090.12
C3_3	10.00	0.63	196.94	-2399.94
C3_4	-39.78	0.10	196.94	-2460.39
C3_5	-35.13	0.20	18.33	-8447.28
C3_6	-22.13	20.00	18.33	-8425.44
C3_7	346.00	20.00	18.33	-7903.48
C3_8	232.14	0.20	18.33	-8012.56
SW_1	15.00	0.10	3623.51	-15930.96
SW_2	15.03	0.50	3623.51	-15930.44
SW_3	15.03	0.50	3137.45	-15930.44
SW_4	5.00	0.50	3137.45	-15973.76
SW_5	15.03	0.50	486.06	-15930.44
SW_6	5.00	0.50	486.06	-15973.76
EG_In	351.00	0.11	26.80	333.49
EG_Out	1.49	0.10	26.80	-23.57

For R134a, the net output of the secondary Rankine cycle was maximized at $max(\dot{W}_{net2,EG}) = 2.103$ MW when the pressure was 19.00 MPa and the mass flow rate was 17.22 kg/s at the turbine inlet C3_7. Besides, in case of the R245fa, the secondary Rankine cycle showed the maximum net output $max(\dot{W}_{net2,EG}) = 1.696$ MW when the pressure was 20.00 MPa and the mass flow rate was 18.33 kg/s at the turbine inlet C3_7. The value of the maximum net power was reduced to 10.4% for the R134a and 24.1% for the R245fa, respectively, compared to that of the propane. Therefore, this indicates that the additional investigation about the effect of various working fluids on the optimization of the secondary Rankine cycle is also required.

4. Conclusions

For the LNG-FSRU vessel, waste heat recovery systems of the type A, B and C have been proposed for generating power from the cold energy of LNG and the heat of exhaust gas during the regasification process. The thermodynamic characteristics were investigated for the type A in which the primary Rankine cycle was applied for the first-stage heat exchanger, the type B in which the secondary Rankine cycle using seawater as its heat source was serially inserted between the first- and second-stage heat exchangers, and the type C in which the heat source for the secondary Rankine cycle was replaced with the exhaust gas from the diesel generators. Notable conclusions of the present study are as follows.

(1) The maximum net output produced by the type A was $max(\dot{W}_{net1}) = 9.728$ MW. The maximum net output additionally produced by the secondary Rankine cycle of the type B, applying seawater as the heat source, was $max(\dot{W}_{net,SW}) = 1.142$ MW as an increase of net power by approximately 11.74% compared to the type A. In the type C, the secondary Rankine cycle replaced the heat source with exhaust gas; the maximum output was $max(\dot{W}_{net2,EG}) = 2.347$ MW, approximately two times the maximum output of the secondary Rankine cycle of the type B.

(2) When comparisons were made for the efficiencies of the 1st and 2nd laws of thermodynamics in cases where the three types of waste heat recovery system had the maximum net outputs, the thermal efficiencies of the type A, B, and C showed an increasing trend with $\eta_I = 0.0590$, $\eta_{I,SW} = 0.0654$, and $\eta_{I,EG} = 0.0741$, respectively.

(3) The results for type C, in which the thermal efficiency was relatively high, suggested the feasibility of the application of the integrated heat recovery system combining the cold energy of LNG and the heat of exhaust gas in the FSRU.

(4) Additionally, for the type C, the necessity was found for continuing future studies on optimization of waste heat recovery for the second-stage heat exchanger and its system, including a variety of the organic working fluids.

Acknowledgment

Nomenclature———————————————————

$\dot{Q}$: Heat transfer rate
C3 : Propane
FPSO : Floating production storage & offloading
FSRU : Floating storage & regasification unit
H : Enthalpy
h : Specific enthalpy
LNG : Liquefied natural gas
$\dot{m}$: Mass flow rate
η_C : Carnot efficiency
NG : Natural gas
η_I : 1st law efficiency
η_{II} : 2nd law efficiency
$\dot{W}$: Power

Subscripts

EG : Exhaust gas (Type C)
K-100 : Turbine in the primary Rankine cycle

K-101   : Turbine in the secondary Rankine cycle
LNG-101: Second-stage heat exchanger
net1   : Net output for the primary Rankine cycle (Type A)
net2   : Net output for the secondary Rankine cycle
P-101   : Pump in the primary Rankine cycle
P-102   : Pump for the vaporizers
P-103   : Pump in the secondary Rankine cycle
Q1   : Vaporizer in the primary Rankine cycle
Q2   : Vaporizer in the secondary Rankine cycle
SW   : Seawater (Type B)

References

[1] V. L. Rocca, Cold recovery during regasification of LNG part one: cold utilization far from the regasification facility, *Energy*, 35 (5) (2010) 2049-2058.

[2] J. Szargut and I. Szczygiel, Utilization of the cryogenic exergy of liquid natural gas (LNG) for the production of electricity, *Energy*, 34 (7) (2009) 827-837.

[3] I. H. Choi, S. Lee, Y. Seo and D. Chang, Analysis and optimization of cascade Rankine cycle for liquefied natural gas cold energy recovery, *Energy*, 61 (2013) 179-195.

[4] X. Shi, B. Agnew, D. Che and J. Gao, Performance enhancement of conventional combined cycle power plant by inlet air cooling, inter-cooling and LNG cold energy utilization, *Appl. Therm. Eng.*, 30 (2010) 2003-2010.

[5] T. S. Kim and S. T. Ro, Power augmentation of combined cycle power plants using cold energy of liquefied natural gas, *Energy*, 25 (9) (2000) 841-856.

[6] K. Kaneko, K. Ohtani, Y. Tsujikawa and S. Fujii, Utilization of the cryogenic exergy of LNG by a mirror gas-turbine, *Appl. Energy*, 79 (4) (2004) 355-369.

[7] T. Miyazaki, Y. T. Kang, A. Akisawa and T. Kashiwagi, A combined power cycle using refuse incineration and LNG cold energy, *Energy*, 25 (7) (2000) 639-655.

[8] J. Wang, Z. Yan, M. Wang and Y. Dai, Thermodynamic analysis and optimization of an ammonia-water power system with LNG (liquefied natural gas) as its heat sink, *Energy*, 50 (1) (2013) 513-522.

[9] G. Oliveti, N. Arcuri, R. Bruno and M. D. Simone, A rational thermodynamic use of liquefied natural gas in a waste incinerator plant, *Appl. Therm. Eng.*, 35 (1) (2012) 134-144.

[10] C. Dispenza, G. Dispenza, V. L. Rocca and G. Panno, Exergy recovery during LNG regasification: electric energy production—Part one, *Appl. Therm. Eng.*, 29 (2009) 380-387.

[11] C. Dispenza, G. Dispenza, V. L. Rocca and G. Panno, Exergy recovery during LNG regasification: electric energy production—Part two, *Appl. Therm. Eng.*, 29 (2009) 388-399.

[12] J. Wang, J. Wang, Y. Dai and P. Zhao, Thermodynamic analysis and optimization of a transcritical CO_2 geothermal power generation system based on the cold energy utilization of LNG, *Appl. Therm. Eng.*, 70 (2014) 531-540.

[13] A. Franco and C. Casarosa, Thermodynamic analysis of direct expansion configurations for electricity production by LNG cold energy recovery, *Appl. Therm. Eng.*, 78 (2015) 649-657.

[14] H. Liu and L. You, Characteristics and applications of the cold heat exergy of liquefied natural gas, *Energy Convers. Manage.*, 40 (1999) 1515-1525.

[15] California State Lands Commission, *Final Environmental Impact Report for Cabrillo Port LNG Deepwater Port License Application*, Appendix G2-1 FSRU Emissions Summary Index (2007).

[16] WARTSILA Engines, *WARTSILA 50DF Product Guide* (2012).

[17] Aspen Technology, *Aspen HYSYS User Guide v7.3* (2011).

[18] D. Y. Peng and D. B. Robinson, A new two-constant equation of state, *Ind. Eng. Chem. Fundam.*, 15 (1) (1976).

[19] F. Dauber and R. Span, *Influence of thermodynamic-property models on the simulation of LNG evaporation and liquefaction processes*, IGRC, Paris (2008).

[20] B. C. Choi and Y. M. Kim, Thermodynamic analysis of a dual loop heat recovery system with trilateral cycle applied to exhaust gases of internal combustion engine for propulsion of the 6800 TEU container ship, *Energy*, 58 (2013) 404-416.

Sangick Lee received the B.S. and M.S. from the Department of Oceanography, Seoul National University, Seoul, Korea, in 1999 and 2001, respectively. He received Ph.D. from the Department of Ocean Systems Engineering, Korea Advanced Institute of Science and Technology (KAIST), Daejeon, Korea, in 2014. He is currently a senior researcher in R&D Center, Korean Register of Shipping. His research interests include process systems engineering and risk, reliability and safety of systems.

Byung Chul Choi earned the B.S. and M.S. in Mechanical Engineering from Korea Maritime University, in 2002 and 2004, respectively. In 2010, he earned a Ph.D. in Mechanical Engineering from Seoul National University. He joined the Department of Mechanical Engineering at Massachusetts Institute of Technology in 2015 as a visiting research scholar. His research interest includes the areas of fundamentals of combustion, internal combustion engine, thermal energy conversion & storage and fire & explosion safety.